arXiv:1110.2922v1 [cond-mat.mtrl-sci] 13 Oct 2011

The phase diagram of $Sr_{1-x}Eu_xTiO_3$: Crossover from displacive to order-disorder dynamics

Z. Guguchia,[1] A. Shengelaya,[2] H. Keller,[1] J. Köhler,[3] and A. Bussmann-Holder[3]

[1]*Physik-Institut der Universität Zürich, Winterthurerstrasse 190, CH-8057 Zürich, Switzerland*

[2]*Department of Physics, Tbilisi State University, Chavchavadze 3, GE-0128 Tbilisi, Georgia*

[3]*Max-Planck-Institut für Festkörperforschung, Heisenbergstr. 1, D-70569 Stuttgart, Germany*

The phase diagram of $Sr_{1-x}Eu_xTiO_3$ is determined experimentally by EPR measurements and analyzed theoretically in terms of the self-consistent phonon approximation (SPA) as a function of x (x=0.0, 0.03, 0.25, 0.5. 0.75, 1.0). It is observed that the oxygen octahedral tilting instability temperature T_S increases nonlinearly with x. The theoretical analysis demonstrates that a crossover from displacive to order-disorder dynamics takes place for $x \geq 0.25$, signaled by a change in the local double-well potential and the soft mode temperature dependence.

PACS numbers: 74.20.Mn, 74.25.Ha, 74.70.Xa, 76.75.+i

The Eu and Sr titanites have a variety of aspects in common which might enlarge their potential applicational properties as mixed crystals or as layered materials. Since Eu and Sr have the same ionic radii and the same valencies in the perovskite ABO_3 structure, also the lattice constants are the same. In addition, both compounds show an incipient ferroelectric instability which is suppressed by quantum fluctuations [1], where the extrapolated values for the polar instability are 37K for $SrTiO_3$ (STO) [2–4] and less than -150K for $EuTiO_3$ (ETO) [5, 6]. Very recently we have shown theoretically and experimentally [7] that a novel analogy exists between both compounds, namely, an oxygen octahedra rotational instability related to the softening of an acoustic phonon mode. The respective transition temperatures T_S differ distinctively, however, namely, T_S=105K in STO, and T_S=282K in ETO. The large gap in T_S between ETO and STO has motivated us to construct the phase diagram of $Sr_{1-x}Eu_xTiO_3$ as a function of Eu content x. Since our previous analysis of the dynamical properties of both systems has been based on the *same* lattice dynamical parameters, with the distinction that the self-consistently derived double-well potentials are very different, i.e. STO is in the displacive limit whereas ETO obeys order-disorder dynamics, we use the same parameters also for the mixed crystals. As data for the soft mode temperature dependence are missing, we employ x-dependent averages of the nonlinear potential for the in between lying compounds. In order to obtain agreement with the experimental phase diagram, the coupling between the oxygen octahedra is varied to reproduce the experiment. The experimental phase diagram has been determined by electron paramagnetic resonance (EPR) where the structural transition temperature T_S appears as a distinct line width anomaly.

The low temperature antiferromagnetic transition of ETO at T_N=5.5K [8] is also x-dependent, but this will not be discussed here where the focus is exclusively on the x-dependent structural instability.

Samples of $Sr_{1-x}Eu_xTiO_3$ have been prepared analogous to the pure compounds as described in Ref. [7]. The values of x are x=0.03, 0.25, 0.5, 0.75, 1, which is sufficient to characterize the phase diagram. The polycrystalline samples have been measured by means of electron paramagnetic resonance (EPR) techniques with the emphasis on investigating and characterizing the structural instability in detail. EPR measurements were performed in a Bruker EMX spectrometer at X-band frequencies ($\nu \approx 9.4$ GHz) equipped with a continuous He gas-flow cryostat in the temperature range $4.2 < T < 300$ K. In this paper we restrict the discussion to temperatures $T > 50$ K. EPR detects the power P absorbed by the sample from the transverse magnetic microwave field as a function of the static magnetic field H. The signal-to-noise ratio of the spectra is improved by recording the derivative dP/dH using a lock-in technique with field modulation. That the EPR method is very powerful for the detection of T_S has been proven early on for STO where a broadening of the EPR line width of a Fe^{3+}-oxygen vacancy pair (V_O) center at T_S has been observed [9]. In the present experiment due to the large Eu spins and the fact that polycrystalline materials were used, only the change of the EPR line width with temperature was studied.

Figure 1 shows the EPR spectra of $Sr_{1-x}Eu_xTiO_3$ with $0.03 \leq x \leq 1$ at T=300 K. For all x one observes a single weakly asymmetric resonance line which is well described by a Dyson shape [10],

$$P(H) = \frac{\triangle H + \alpha(H - H_{res})}{(H - H_{res})^2 + \triangle H^2} \qquad (1)$$

i.e., a Lorentz line at resonance field H_{res} with half width at half maximum ΔH and a contribution $0 \leq \alpha \leq 1$ of dispersion to the absorption, resulting in a characteristic asymmetry. The dispersion contribution to the EPR line shape evidences that the samples are conducting, since the asymmetric signal is typical for metals where the skin effect drives electric and magnetic components of the microwave field out of phase. The parameter α depends on sample size, geometry, and skin depth. If the skin depth is small as compared to the sample size, α approaches

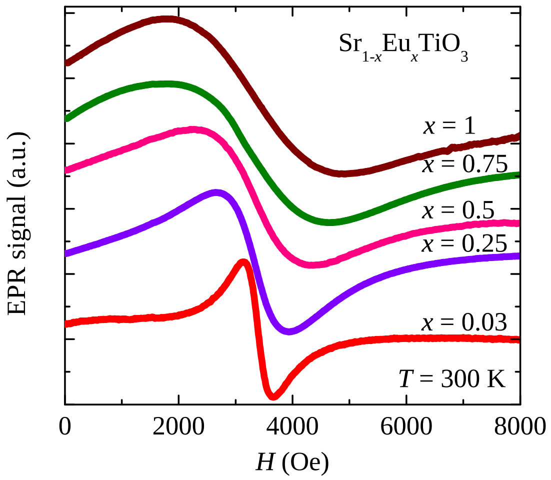

FIG. 1: (Color online) EPR spectra of Eu^{2+} in $\mathrm{Sr}_{1-x}\mathrm{Eu}_x\mathrm{TiO}_3$ for $0.03 \leq x \leq 1$ at T=300K.

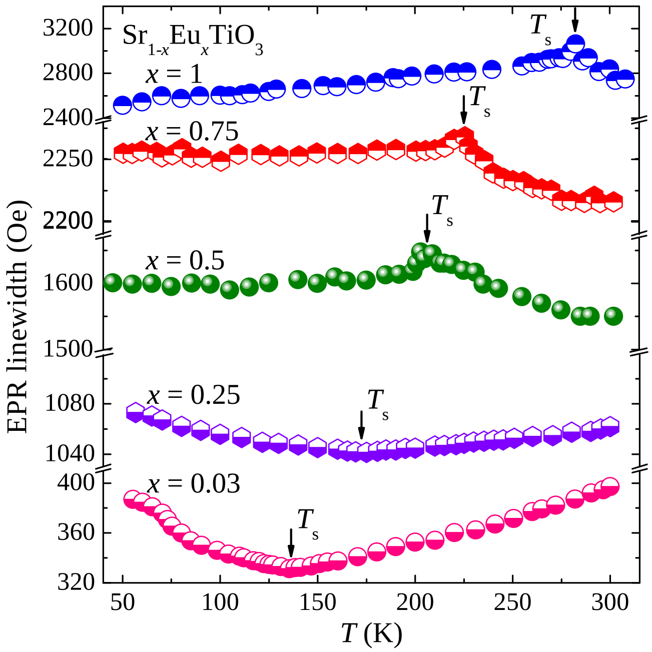

FIG. 2: (Color online) Temperature dependence of the EPR linewidth for $\mathrm{Sr}_{1-x}\mathrm{Eu}_x\mathrm{TiO}_3$ samples with $0.03 \leq x \leq 1$. The arrows indicate the structural phase transition temperature.

1. From Fig. 1 it is obvious that the EPR signal broadens with increasing Eu concentration. This effect can be explained by an increasing magnetic dipolar interaction between Eu^{2+} ions as their average distance is reduced with increasing Eu concentration. The Lorentzian line shape is a signature of the exchange narrowing process due to strong exchange coupling between the magnetic Eu^{2+} ions. The fine and hyperfine structures, which are expected for the single Eu^{2+} ions, are not observed in our samples. This implies that starting from the smallest Eu concentration x=0.03 studied here, the exchange narrowing process is sufficient to merge the entire spectrum into a single EPR line. Figure 2 shows the temperature dependence of EPR line width in $\mathrm{Sr}_{1-x}\mathrm{Eu}_x\mathrm{TiO}_3$ samples with $0.03 \leq x \leq 1$. For x=1 and in the temperature interval 50-285 K, the EPR line width broadens linearly with a slope of approximately 0.2 mT/K. The linear temperature dependence is characteristic for the Korringa mechanism of relaxation where localized Eu^{2+} moments couple to charge carriers through an exchange interaction [10]. In this case the slope of the linear broadening is proportional to $(J_{\mathrm{Eu-CE}}\mathrm{N}(E_{\mathrm{F}}))^2$, where $\mathrm{N}(E_{\mathrm{F}})$ is the conduction electron density of states at the Fermi energy, and $J_{\mathrm{Eu-CE}}$ is the exchange coupling constant of the Eu spins with the conduction electron (CE) spins [10]. It is obvious from Fig. 2, that the EPR line width exhibits an anomaly at 285K. This temperature coincides with specific heat anomaly due to the structural phase transition recently observed in EuTiO_3 [7]. Qualitatively the sensitivity of the EPR line width to the structural phase transition can be understood as stemming from either band structure modifications $\mathrm{N}(E_{\mathrm{F}})$ or from changes of $J_{\mathrm{Eu-CE}}$. As can be seen in Fig. 2, the EPR line width in EuTiO_3 starts to increase with decreasing temperature above T_{S} suggestive of conductivity changes above the structural phase transition. At T_{S} this behavior changes abruptly and an almost linear decrease with decreasing T is seen. For the compositions x=0.75 and 0.5 an analogous behavior is observed with T_{S} moving to lower temperatures. The results are shown in Fig. 2. It is interesting to note that the maximum of the EPR line width changes to minimum as a function of temperature below x=0.25. Although the reason for this is not clear at present, tentative explanations are given below.

The phase diagram as deduced from Figure 2 is shown in Figure 3. Obviously T_{S} depends nonlinearly on x.

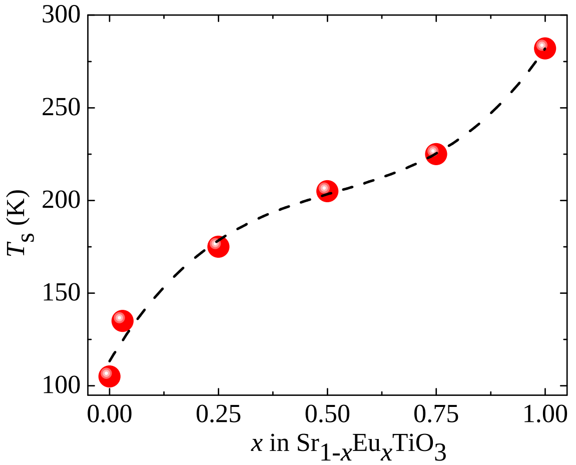

FIG. 3: (Color online) Temperature dependence of the EPR linewidth for $\mathrm{Sr}_{1-x}\mathrm{Eu}_x\mathrm{TiO}_3$ samples with $0.03 \leq x \leq 1$. The arrows indicate the structural phase transition temperature.

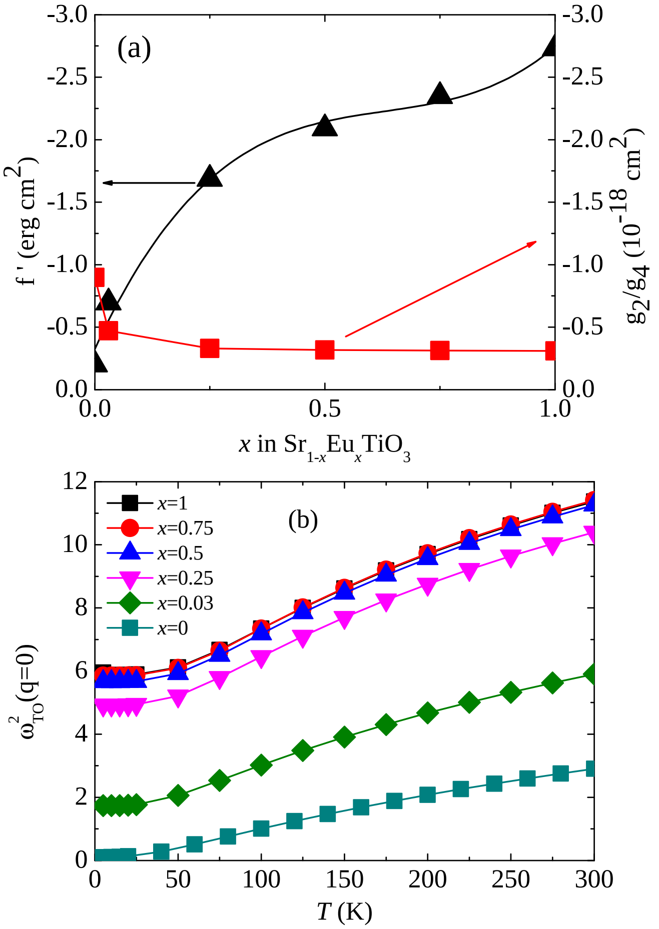

FIG. 4: (Color online) (a) The x-dependence of the octahedral coupling f' (triangles) and the double-well potential height g_2/g_4 (squares). (b) Temperature and x-dependence of the soft optic mode frequency where the color code for the different x-values is given in the figure.

For $x \leq 0.25$ T_S increases sharply to become almost proportional to x between $0.25 \leq x \leq 0.75$ followed by a steep increase for $x \geq 0.75$. This nonlinear dependence is rather unexpected since the ionic sizes of Sr and Eu are the same, and these ions are not involved in the TiO_6 rotational instability. However, as we have shown recently [7], the dynamics of the phase transitions of STO and ETO differ considerably, being almost displacive for STO and of order-disorder type for ETO. It can thus be assumed that a crossover between both dynamics is present in the mixed crystals which causes the non-monotonic dependence of T_S on x.

In order to model the phase diagram of STO-ETO we adopt the same nonlinear polarizability framework as previously used [7, 11–13], and employ x-dependent averages of the double-well defining quantities g_2,g_4 where g_2 is the attractive harmonic electron-ion interaction parameter and g_4 the nonlinear fourth order repulsive term. These values are typically derived self-consistently from the soft optic mode frequency. The lack of data from the mixed crystals does not admit to follow the same procedure. The x-dependent double-well potential parameters are given in terms of the barrier well g_2/g_4 and are shown in Figure 4a. Obviously, around $x \geq 0.25$ the barrier height becomes independent of x, whereas for $x \leq 0.25$ a strong x-dependence sets in. Since ETO is in the order-disorder limit and STO in the displacive limit, x=0.25 represents the border where a dynamical crossover between both takes place. This can also been seen from the temperature and x-dependence of the long wave length soft optic mode (Figure 4b) where for $x > 0.25$ all modes fall almost on the same line and follow the same temperature dependence. Since at the same Eu composition also the line width anomaly changes from peak to dip, we identify this crossover as its origin. Details will be given elsewhere. With the double-well defining parameter values and the temperature dependence of the long wave length optic mode frequencies it is possible to deduce the temperature dependence of the zone boundary related acoustic mode energy corresponding to the octahedral rotational instability [13]. This alone is, however, not enough to reproduce the experimental data for T_S. It is necessary to also correct for the spin-phonon coupling which - as has been shown previously [7] - strongly suppresses the zone boundary acoustic mode frequency. We infer this correction indirectly by modifying the second nearest neighbor coupling f' such as to yield the correct T_S. Interestingly, we find that this coupling follows the x dependence of T_S (Figure 4a).

To summarize, the phase diagram of $Sr_{1-x}Eu_xTiO_3$ has been determined experimentally by EPR measurements with focus on the structural instability related to oxygen octahedral tilting. It is found that this instability depends nonlinearly on the Eu composition x. The theoretical analysis is based on the nonlinear polarizability model and predicts a crossover in the critical dynamics around x=0.25. The experimental phase diagram is reproduced by assuming that the double-well potential represents a doping and x dependent average of the end member potentials and by adjusting the next nearest neighbor interactions which are found to follow the x-dependence of T_S. From the calculations it is expected that for $x \leq 0.25$ also anomalies in the acoustic mode dispersion appear which can be detected experimentally by resonant ultrasound spectroscopy and as precursor dynamics in local probe experiments, analogous to STO.

This work was supported by the Swiss National Science Foundation, the SCOPES grant No. IZ73Z0_128242, the NCCR Project MaNEP, the EU Project CoMePhS, and the Georgian National Science Foundation grant GNSF/ST08/4-416.

[1] K.A. Müller, and H. Burkhard, Phys. Rev. B **19**, 3593 (1979).

[2] H. Burkhard and Müller, Helv. Phys. Acta **49**, 725 (1976).

[3] H. Uwe and T. Sakudo, Phys. Rev. B **13**, 271 (1976).

[4] W. Cochran, Adv. Phys. **3**, 387 (1960).

[5] S. Kamba, D. Nuzhnyy, P. Vaněk, M. Savinov, K. Knižek, Z. Shen, E. Santavá, K. Maca, M. Sadowski, and J. Petzelt, Europhys. Lett. **80**, 27002 (2007).

[6] V. Goian, S. Kamba, J. Hlinka, P. Vaněk, A. A. Balik, T. Kolodiazhnyi, and J. Petzelt, Europ. Phys. J. B **71**, 429 (2009).

[7] A. Bussmann-Holder, J. Köhler, R. K. Kremer, and J. M. Law, Phys. Rev. B **83**, 212102 (2011).

[8] T. R. McGuire, M. W. Shafer, R. J. Joenk, H. A. Halperin, and S. J. Pickart, J. Appl. Phys. **37**, 981 (1966).

[9] Th. Von Waldkirch, K. A. Müller, and W. Berlinger, Phys. Rev. B **7**, 1052 (1973).

[10] S.E. Barnes Adv. Phys. **30**, 801 (1981).

[11] R. Migoni, H. Bilz, and D. Bäuerle, Phys. Rev. Lett. **37**, 1155 (1976).

[12] H. Bilz, G. Benedek, and A. Bussmann-Holder, Phys. Rev. B **35**, 4840 (1987).

[13] A. Bussmann-Holder, H. Büttner, and A. R. Bishop, Phys. Rev. Lett. **99**, 167003 (2007).